Seismic behavior of reinforced concrete bridge columns with Copper-based SMA and ECC

Sebastian Varela[1] and M. 'Saiid' Saiidi[2]

[1] PhD Candidate, Dept. of Civil and Environmental Engineering, University of Nevada, Reno, NV, USA
[2] Professor, Dept. of Civil and Environmental Engineering, University of Nevada, Reno, NV, USA

ABSTRACT: Advanced materials such as engineered cementitious composite (ECC) and superelastic shape memory alloys (SMAs) have been found to be effective in reducing damage and increasing the serviceability of bridge columns after strong earthquakes. Previous studies in which SMA has been used for seismic applications have made use of Nickel-Titanium (NiTi) SMA, which despite its excellent superelastic properties can be very expensive to use in the practice. A recently-developed Copper-Aluminum-Manganese (CuAlMn) superelastic SMA has been reported to have comparable superelastic properties to most NiTi SMAs at only a fraction of their cost, and is therefore expected to be more easily adopted in the practice. As part of a major project funded by the U.S. National Science Foundation, a quarter-scale bridge column model using superelastic CuAlMn SMA and ECC in the plastic hinge region was designed, constructed and tested dynamically on a shake table under near-fault motions. The novel materials that were used mitigated column damage, residual drift and loss of lateral and vertical load capacity even when subjecting the column model to a maximum drift ratio of 12%. Based on experimental and analytical results it was concluded that using ECC and CuAlMn SMA could be a feasible alternative to resist intense earthquakes while keeping concrete bridges functional.

1 INTRODUCTION

Reinforced concrete bridges (RC) are critical links in any major ground transportation network and therefore in the event of failing after a strong earthquake they could cripple the entire transportation system. Direct monetary losses associated with repair or replacement of bridge structures along with indirect losses related to business disruption arising from traffic delays and detours due to bridge downtime can greatly affect the economy of a region. Modern seismic design guidelines for standard RC bridge columns rely on the use of special reinforcement detailing rules and requirements for minimum ductility capacity of structural members to ensure plastic behavior and energy dissipation will take place during strong earthquakes. Although these guidelines result in structures having lower initial cost in comparison to a structure that is designed to behave elastically, they do not specifically address the functionality of the bridge as they are aimed mainly to minimize damage under moderate earthquake ground motions, and to prevent collapse under rare earthquakes resulting in high levels of ground shaking, AASHTO (2011). Consequently, under the design event the bridge is very likely to suffer significant damage and disruption to service, and may require partial or complete replacement, thereby increasing costs in the long term.

One possible strategy to mitigate damage to reinforced concrete bridge columns in regions of high seismicity is to make use of advanced materials that are able to accommodate large earthquake displacement demands without undergoing the typical severe damage expected from conventional RC members. Two of such advanced materials are Engineered Cementitious Composite (ECC) and superelastic shape memory alloys (SMAs). ECC is a grout-like material that consists of fine aggregates, Portland cement, special admixtures, and Polyvinyl Alcohol (PVA) fibers that give it superior ductility in tension and compression. These properties have been found to help in significantly reducing the extent of apparent damage in the plastic hinge region and lateral load degradation of concrete bridge columns as demonstrated in the studies by Varela and Saiidi (2014), Saiidi and Wang (2006), Saiidi et al. (2009), Cruz-Noguez and Saiidi (2013), and Varela and Saiidi (2015), amongst others. On the other hand, SMAs are materials that have the unique ability to undergo large deformations and recover their shape either through heating (shape memory effect) or upon stress removal (superelastic effect). Nickel-Titanium (NiTi) superelastic SMA used in the form of longitudinal reinforcing bars inside the plastic hinge region of bridge columns has been found to be effective in reducing the residual drifts of the columns after intense earthquake loading, Saiidi and Wang (2006), Saiidi et al. (2009), Cruz-Noguez and Saiidi (2013), Varela and Saiidi (2014b). This is because this type of alloy displays a flag-shaped hysteretic behavior that provides self-centering to the columns, meaning these columns could stay functional after being subjected to a strong earthquake. However, due to the large strains that SMA is able to undergo, it is necessary to use it in combination with ECC in order to further reduce damage, residual drifts and loss of capacity as observed by Saiidi et al (2009).

Although previous studies have demonstrated the good performance of bridge columns with NiTi SMA and ECC, it can be expensive to use NiTi in the practice due to the high cost of Titanium, an absence of established bridge engineering market, and because NiTi is very difficult to machine. An emerging Copper-Aluminum-Manganese (CuAlMn) superelastic SMA has been reported to have comparable superelastic properties to most NiTi SMAs at only a fraction of the cost due to relatively lower cost of Copper, lower production cost, and easier machinability. In the study by Varela and Saiidi (2014) CuAlMn SMA bars were used at a larger scale for the first time. In that study, a quarter-scale Cast-In-Place reinforced concrete column model using superelastic CuAlMn SMA and ECC in the plastic hinge region was designed, constructed, and tested dynamically on a shake table under near-fault ground motions. The main objective of their study was to experimentally evaluate the earthquake performance of this innovative bridge column model detailed according to modern seismic design requirements. This paper summarizes the main findings of the experimental and analytical investigation by Varela and Saiidi (2014) as well as findings from recent analytical studies addressing the implications of using low energy dissipation CuAlMn SMA reinforcing bars in the seismic performance of concrete bridge columns.

2 EXPERIMENTAL STUDIES ON THE SEISMIC BEHAVIOR OF NOVEL BRIDGE COLUMNS WITH CUALMN SMA AND ECC: VARELA AND SAIIDI (2014).

2.1 Model description

The elevation and cross section views of the quarter-scale model tested by Varela and Saiidi (2014) are shown in Fig. 1. The column footing and head were made of conventional reinforced concrete and were designed to stay elastic throughout the testing. The model was designed to be tested in a cantilevered, single-curvature configuration. The longitudinal and transverse steel in the column were proportioned to be representative of those for circular bridge columns in the practice. ECC and CuAlMn SMA were used in the plastic hinge region at the lower part of the column, as shown in Fig. 1. The SMA bars were connected to the column's longitudinal reinforcement above and below the plastic hinge region using threaded couplers. A target axial load index (ALI) -defined as the ratio of the applied axial load to the product of the gross cross-sectional area and the specified concrete compressive strength - of about 7% was selected, as this is within typical ALIs for RC bridge columns in the practice. An aspect ratio (height/diameter) of around 4.5 was selected to ensure the behavior of the model would be dominated by flexure.

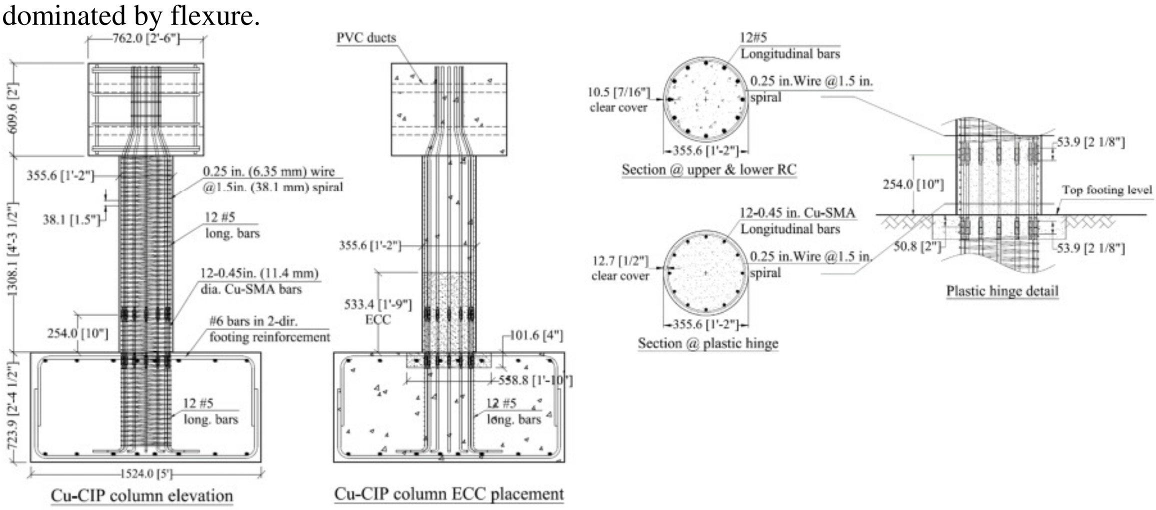

Figure 1. Quarter-scale column model dimensions and details.

2.2 *Materials*

Inside the plastic hinge region, ECC with specified compressive strength of 42 MPa (6.0 ksi) at 28 days was used. The measured ECC compressive strength on the column test day was 54 MPa (7.7 ksi). Normal-weight concrete with specified strength of 35 MPa (5.0 ksi) was used in the footing and the rest of the column. The measured compressive strength of the concrete in the footing and top of the column on the day the column was tested was 38.5 MPa (5.5 ksi) and 45.5 MPa (6.5 ksi), respectively. ASTM A-615 Grade 60 (420 MPa) mild steel reinforcing bars were used throughout the column except for the transverse reinforcement spiral wire, which had an average yield strength of 350 MPa (50 ksi). Round, superelastic CuAlMn SMA bars with a material composition of $Cu_{71.6}Al_{17}Mn_{11.4}$ were produced by Furukawa Techno Material Co., Ltd. (Hiratsuka, Kanagawa-Japan) and were machined to a total length of 304.8 mm (12 in.) and a dog-bone shape with 11.43 mm (0.45 in.) diameter in the middle portion and 9/16"-18 UNF threads 38.1 mm (1.5 in.) long at the ends. Results from tensile testing of one of these bars are shown in Fig. 2, along with the measured hysteretic parameters based on the nonlinear model for SMA proposed by Tazarv and Saiidi (2014).

2.3 *Testing procedure*

The column model was tested on a shake table at the Earthquake Engineering Laboratory at the University of Nevada, Reno, as shown in Fig. 3. Ground motions were uniaxial and were applied along the N-S direction of the laboratory, as indicated in Fig. 3. The Rinaldi Receiving Station near-fault record from the 1-17-1994 Northridge, California earthquake was simulated in order to maximize the chances of causing residual displacements to the model. The time axis in the acceleration record was compressed by a factor of $1/\sqrt{4}$ to account for geometric scaling of the model. Amplitude scaling factors that were determined from pre-test analyzes were applied incrementally to the ground motion to study the full hysteretic behavior of the model up to failure. Further details about the design and construction as well as testing procedure can be found in Varela and Saiidi (2014).

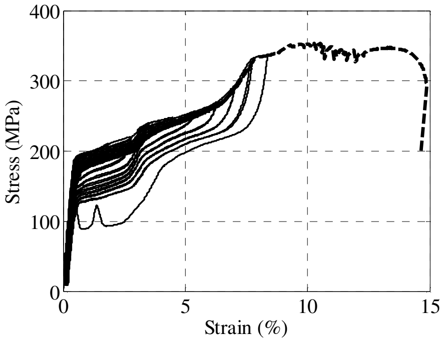

Parameter name	Symbol	Value
Yield (forward transf.) stress	f_y, MPa [ksi]	168 [24]
Ultimate stress	f_u, MPa [ksi]	350 [50]
Elastic modulus	k_1, GPa [ksi]	31.5 [4500]
Post-yield modulus	k_2, GPa [ksi]	1.96 [280]
Ratio of forward to reverse transformation stress	β	0.2
Superelastic strain	ε_r (%)	7
Rupture strain	ε_u (%)	14

Figure 2. Hysteretic tensile behavior and nonlinear parameters of a sample 11.43 mm (0.45 in.) CuAlMn SMA bar.

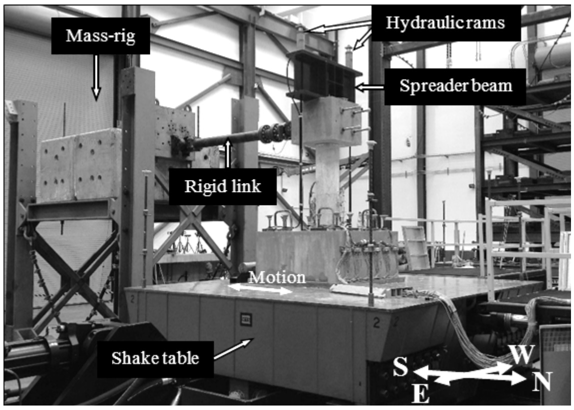

Figure 3. Shake table test setup.

2.4 *Key test results*

The apparent damage state at the North and South sides of the column after the last earthquake run of 1.57 x Rinaldi, equivalent to 450% times the 'design' level earthquake (PGA=1.31 g) is shown in Fig. 4. Damage consisted of multiple fine tensile cracks and a single larger crack at the north side of the column, and minor compressive spalling of the ECC cover at the column-footing interface at the south side of the column. Removal of cover ECC after testing revealed that two SMA bars ruptured in a ductile manner at the dog-bone section, and that no distress in any of the longitudinal mild steel bars or threaded couplers occurred. Furthermore, it was concluded from strain gage data, curvature measurements and test observations that all nonlinear behavior in the column took place in the plastic hinge zone only, and the plastic hinge length was found to be equal to roughly one half of the SMA length above the footing or 127 mm (5 in.). The plastic hinge region of a structural member is defined as that where substantial inelastic behavior takes place under extreme loading, and along which the nonlinear curvature distribution is assumed to be constant for ease of nonlinear force and displacement capacity calculations. All of the results indicated that CuAlMn SMA and ECC significantly reduced the extent of apparent damage of the column, as it had been found in previous studies involving ECC and NiTi SMA.

The column exhibited stable hysteretic behavior with minor loss of capacity even after being subjected to a maximum drift of about 12% during the last earthquake run. Moreover, the residual drift of the model at the end of testing was less than 0.5% proving that CuAlMn SMA was very effective in providing self-centering to the column. However, due to the narrow flag-shaped hysteresis of CuAlMn SMA (see Fig. 2) the column did not dissipate as much hysteretic energy as if it had been reinforced with mild or NiTi SMA bars, raising questions as to how could this potentially affect the seismic performance of concrete columns with CuAlMn SMA and ECC in the practice .

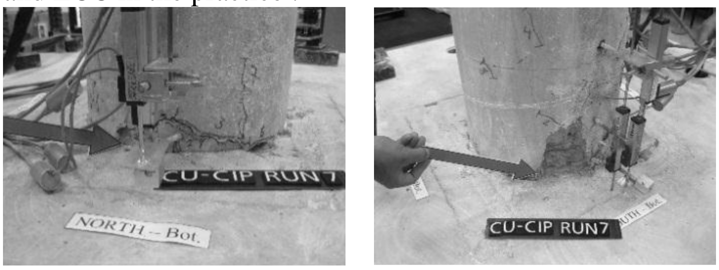

Figure 4. Plastic hinge damage after 12% drift. Left: north side, right: south side.

Post-test analyzes studies using a simple 2-dimensional nonlinear fiber model of the column tested that was developed in OpenSees were able to accurately match some of the key test results such as maximum forces and displacements. Based on the experimental and analytical results it was concluded that using superelastic CuAlMn SMA and ECC in the plastic hinge regions of bridge columns in high seismic zones could be a feasible alternative to keep bridges functional after strong earthquakes.

3 ANALYTICAL STUDIES ON THE SEISMIC PERFORMANCE OF CONCRETE BRIDGE COLUMNS WITH CUALMN SMA AND ECC

3.1 Description of analysis models, motions used and analysis procedure

In order to study the implications of using low energy dissipation CuAlMn SMA reinforcement in the seismic performance of concrete bridge columns, six different cantilever columns were designed and analyzed dynamically under 3 near-fault (NF) and 3 far-fault (FF) motions. The cross-sections of the 6 models are shown in Fig. 5. Three of them were benchmark steel-RC columns with longitudinal reinforcement ratios close to 1%, 2% and 3%, denoted RC1, RC2, and RC3 respectively, and the other three were models with CuAlMn SMA and ECC in the plastic hinge region with comparable reinforcement ratios and the same lateral load capacity at 5% drift as their RC counterparts, and were denoted as SMA_A, SMA_B, and SMA_C. This load matching procedure allowed comparisons to be made between RC columns and ECC/SMA columns. The height of all six columns was assumed to be 6.1 m (20 ft.), which corresponds to an aspect ratio of 5 for the RC columns and of 4 for the ECC/SMA columns. As noted in the paper by Varela and Saiidi (2014), if a force-based approach is considered, columns with ECC and CuAlMn SMA need to have a larger cross section if it is desired to match their capacity with that of conventional RC columns. This is because ECC has lower elastic modulus than normal-weight concrete and CuAlMn SMA has significantly lower yield strength in comparison to steel rebar, and not increasing the column diameter would result in very high reinforcement ratios that could lead to potential congestion and constructive issues.

All column sections were designed and detailed according to the 2011 AASHTO Guide specifications for LRFD Seismic Bridge design. The main characteristics of the NF and FF motions used in the analysis are summarized in Table 1. A target design spectrum according to the AASHTO 2009 guide specifications for LRFD seismic bridge design was selected for a hypothetical location in the vicinity of the Olive View-UCLA medical center in Sylmar, California. This is a zone of high seismic hazard that was greatly affected during the 1-17-1994

Northridge Earthquake. The soil type was assumed to be site class D "stiff soil", while the seismic design category (SDC) was taken as D. The motions selected were scaled using the factors reported in the last column of Table 1, which were calculated in order to match the peak ground acceleration (PGA) of each record to that of the target design spectrum, equal to 1g. The AASHTO target design spectrum is representative of a ground motion with a 7% probability of exceedance in 75 years, equivalent to an event with 1000 years return period. A total of 36 analyzes were conducted, corresponding to the six column models subjected to each of the six motions. The columns were analyzed using finite element computer program OpenSees. Each column was modeled as a 2-dimensional force-based distributed plasticity element with a nonlinear fiber section. Appropriate constitutive models for the stress-strain behavior of steel rebar, SMA, concrete and ECC were used. Both material and geometric nonlinearities were included in the analysis. The axial load and seismic weight applied to the models was kept constant at 3,560 kN (800 kips), which is equivalent to a realistic ALI of about 9% for the RC columns and 6% for the ECC/SMA columns.

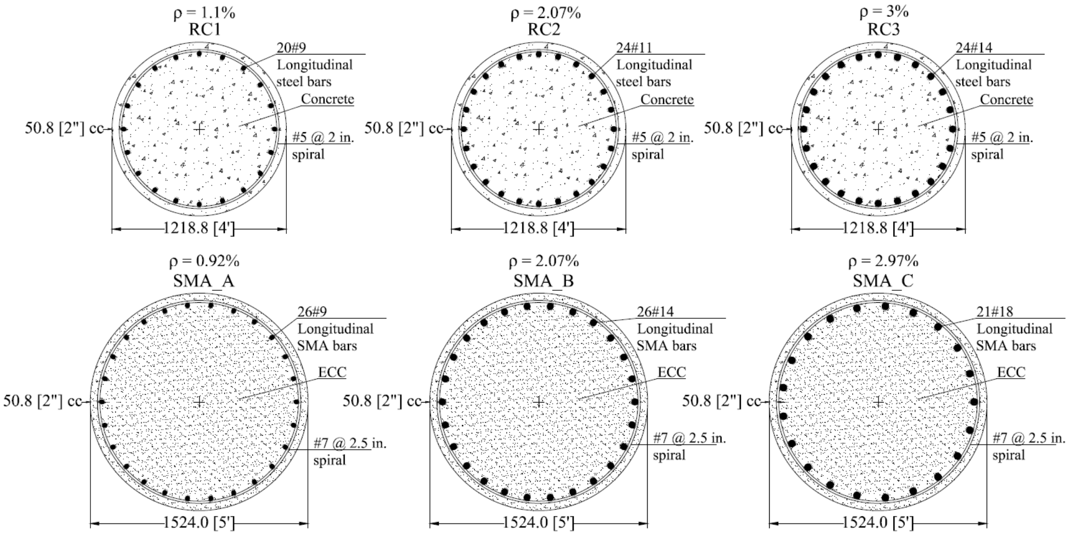

Figure 5. RC and ECC/SMA column sections.

Table 1. Ground motions selected for analysis.

Motion	Event	M_w	Year	Component	Station	R_{rup} (km)	R_{jb} (km)	PGA (g)	Scale factor*
NF1	Northridge-01	6.7	1994	052	Rinaldi Receiving Sta	6.5	0.0	0.612	1.698
NF2	Tabas- Iran	7.3	1978	TR	Tabas	2.0	1.8	0.852	1.221
NF3	Kobe- Japan	6.9	1995	000	KJMA	1.0	0.9	0.579	1.797
FF1	Kern County	7.4	1952	111	Taft Lincoln School	38.9	38.4	0.180	5.768
FF2	San Fernando	6.6	1971	291	Castaic Old Ridge Route	22.6	19.3	0.275	3.782
FF3	Michoacan - Mexico	8.3	1985	NS?	Ciudad Universitaria (CUMV)	N.A.	N.A.	0.038	27.368

*Scaling factor to achieve 100% x DE PGA = 1.0 g

R_{rup} is the closest distance to the coseismic rupture plane

R_{jb} is the closest distance to the surface projection of the coseismic rupture plane

CUMV was recorded on rock at Mexico City, located at least 350 km away from the epicenter.

3.2 *Key analysis results and preliminary observations*

The analytical results were interpreted using four main parameters: the total dissipated Energy (E_d), the inelasticity index (II), the displacement ductility demand (μ_Δ), and the residual drift ratio (Δ_{res}). The dissipated energy is equal to the cumulative area under the load-displacement curve for each column over the total motion duration while the inelasticity index is a measure of the plastic displacement demand (Δ_{max} - $\Delta_{y,eff}$) relative to the total plastic displacement capacity of the column (Δ_u - $\Delta_{y,eff}$) . The maximum *II* is 1 and corresponds to failure, while an *II* of zero indicates the column displacement and force are at the effective yield point and a negative *II* indicates the column is elastic. The effective yield forces and displacements were calculated using customary elasto-plastic bilinear idealizations of the pushover curves of each column. It should be noted that all of these idealizations were elastic-perfectly plastic, except for SMA_B and SMA_C which were more accurately represented with a post-yield hardening branch.

Figure 6a illustrates the calculated *II* for all 36 analyzes conducted. An arbitrary *II* of 1.5 was defined to identify those columns in which excessive geometric nonlinearity occurred and convergence could not be achieved after the models experienced drifts in exceedance of 20%. From Fig. 6a, it is seen that RC columns are likely to be more vulnerable to excessive drifts under near and far fault motions regardless of the reinforcement ratio in comparison to ECC/SMA columns. Although there were a few differences in terms of the *II* for RC and ECC/SMA columns with the same reinforcement ratio, Fig. 6a shows that values for the *II* were comparable between the two for the most part. From Fig. 6b it is seen that ECC/SMA columns tend to experience larger ductility demands than comparable RC columns under NF motions, indicating a potential issue related to the need to control large inelastic displacements in those cases. Increasing the reinforcement ratio seemed to be effective in reducing the ductility demand. On the other hand, for FF motions the ductility demand seemed to be comparable between RC and ECC/SMA models with similar flexural strength.

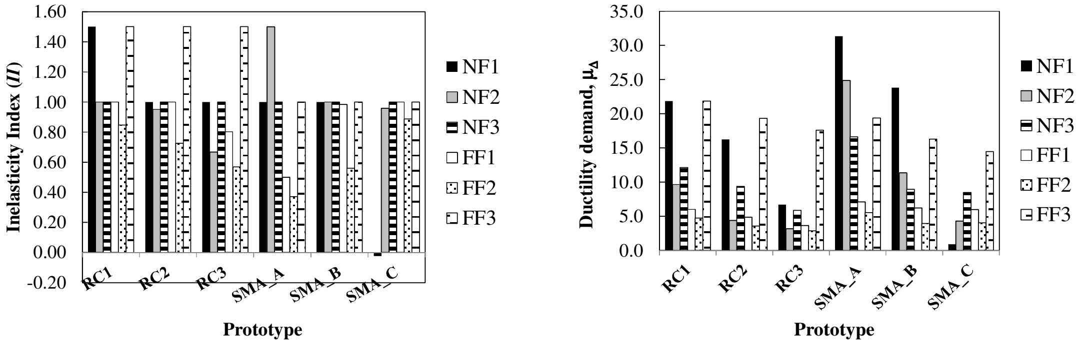

(a) (b)

Figure 6. Calculated inelasticity index and ductility demand for all columns.

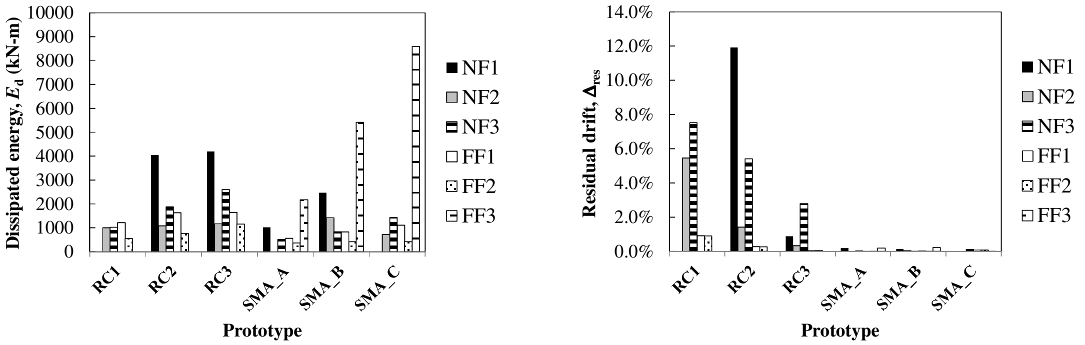

(a) (b)

Figure 7. Calculated dissipated energy and residual drift for all columns.

The amount of energy dissipated as well as the residual drift for each model analyzed is summarized in Figs. 7a and 7b, respectively. In this Figure it is clear that as the reinforcement ratio increased the energy dissipated also increased for both RC and ECC/SMA columns, but as expected the ECC/SMA columns typically dissipated less energy than RC columns with comparable flexural strength under the same ground motion, the only exception being RC2 versus SMA_B under NF2. The self-centering capabilities of SMA were confirmed in Fig. 7b, where it can be seen that even under near-fault motions (which tend to cause very large residual drifts on RC models) ECC/SMA columns had little or no residual drifts. The overall observation of this analytical study was that there was no clear evidence that the low energy dissipation of RC columns with CuAlMn SMA and ECC adversely affected their performance in comparison to that of conventional steel-RC columns.

4 CONCLUSIONS

This paper presented highlights of experimental and analytical investigations on the seismic performance of reinforced concrete bridge columns with copper-based SMA and ECC. Based on results from shake table tests on a quarter-scale column model it was concluded that using CuAlMn and ECC in the plastic hinge region of reinforced concrete columns leads to excellent seismic performance and prevents significant damage to allow bridges to stay functional even after strong earthquakes. These novel materials mitigate column damage, and would therefore help in reducing bridge downtime after earthquakes and associated costs in the long term. Analytical studies indicated that the low energy dissipation capabilities of CuAlMn SMA/ECC columns do not necessarily hinder their seismic performance as it could be comparable or even better than that of steel-RC columns.

5 ACKNOWLEDGMENTS

Special gratitude goes to Dr. Sally Nerlove, the NSF Program Director for the Partnership for Innovation program, for her support and guidance. Furukawa Techno Material Co. of Japan is thanked for generously donating Copper-based SMA bars. Dr. Yoshikazu Araki of Kyoto University in Japan is thanked for his technical input. Thanks are due Mr. Aaron Holmes at the NDOT materials lab for help with rebar testing. The assistance from staff members at the Earthquake Engineering lab at the University of Nevada, Reno is gratefully acknowledged. The material in this paper is based upon work supported by the National Science Foundation under Grant No. IIP-1114406. The UNR shake table site operation and maintenance is funded by NSF Grant No. CMS-0402490.

6 REFERENCES

AASHTO, 2011. *AASHTO Guide Specifications for LRFD Seismic Bridge Design*, American Association of State Highway and Transportation Officials, Washington, DC.

Cruz-Noguez, C., and Saiidi, M., 2013, Performance of advanced materials during earthquake loading tests of a bridge system. *ASCE Journal of Structural Engineering*, 139(1): 144-154.

Saiidi, M., and Wang, H., 2006, An exploratory study of seismic response of concrete columns with shape memory alloys reinforcement. *ACI Structural Journal*, 103(3): 436-443.

Saiidi, M., O'Brien, M., and Zadeh, M., 2009, Cyclic response of concrete bridge columns using superelastic nitinol and bendable concrete. *ACI Structural Journal*, 106(1): 69-77.

Tazarv, M. and Saiidi, M., 2014, Reinforcing NiTi superelastic SMA for concrete structures. *ASCE Journal of Structural Engineering*, 10.1061/(ASCE)ST.1943-541X.0001176, 04014197.

Varela, S., and Saiidi, M., 2014, Dynamic performance of novel bridge columns with superelastic CuAlMn shape memory alloy and ECC. *International Journal of Bridge Engineering (IJBE)*, 2(3): 29-58.

Varela, S., and M. Saiidi, 2014b, Damage-free earthquake-resistant deconstructible columns for ABC. Proceedings, *2014 National Bridge Accelerated Bridge Construction Conference.* Miami, Florida: Accelerated Bridge Construction – University Transportation Center (ABC-UTC).

Varela, S., and M. Saiidi, 2015, Shake table tests on a 2-span bridge model with advanced materials and deconstructible columns. Proceedings, *7th Colombian National Congress on Earthquake Engineering.* Bogota, Colombia: Universidad de los Andes, Asociacion Colombiana de Ingenieria Sismica.